

Charged Polymer Brushes: Counterion Incorporation and Scaling Relations

Heiko Ahrens,¹ Stephan Förster,² and Christiane A. Helm^{1,*}

¹*Institut für Physikalische Chemie, Johannes Gutenberg-Universität, Jakob-Welder Weg 11, D-55099 Mainz, Germany*

²*Max-Planck Institut für Kolloid- und Grenzflächenforschung, Kantstraße 55, D-14513 Teltow, Germany*

(Received 15 April 1998)

Amphiphilic block copolymers consisting of a fluid hydrophobic and a polyelectrolyte part form monolayers at the air/water interface. With x-ray reflectivity it is shown that the hydrophobic block is a nm-thick melt, while the polyelectrolyte forms an osmotically swollen brush of constant thickness, independent of grafting density and with stoichiometric counter ion incorporation. Only at high salt conditions (above 0.1 M), the brush shrinks and the thickness scales with the molecular area and the salt concentration (corrected for excluded volume interactions) with an exponent $-1/3$. [S0031-9007(98)07505-X]

PACS numbers: 61.41.+e

The behavior of polymers adsorbed or anchored to surfaces has been the subject of many studies, both fundamental and applied [1,2]. Indeed, it is important to understand their behavior to control aggregation as well as segregation processes (paper making, water treatment, paint and food industry, separation in the mining industry, medical science, among others). In all these applications, polyelectrolytes adsorb to large surfaces. From a fundamental point of view, it is interesting to describe how the conformation of charged chains immersed in water is changed at interfaces. The simplest imaginable system are polyelectrolyte brushes, where the chains, carrying a significant number of ionizing groups are anchored by one end on a flat surface. Theoretically, this system has been studied intensively, partly as an extension of the well-understood and classical problem of neutral brushes [3,4], partly in the hope that in a restricted geometry the somewhat puzzling behavior of charged chains in solution may be easier to understand [5]. According to theoretical predictions and in contrast to neutral brushes the brush stretching is determined primarily by electrostatic interactions in the layer rather than by sterical repulsion between monomers [6–8]. However, few experiments substantiate this claim [9]. We attach the chains to the air/water interface and can thus easily control the grafting density and the salt concentration in the subphase.

Theoretical background.—For densely tethered chains [cf. schematics in Fig. 1(b)] two different cases can be distinguished, the “osmotically swollen brush” and the “salted brush” [7] depending on the relation of the ion concentration in the brush to the one in solution. All theoretical predictions are based on the assumption that the conformation force of the stretched polymer $f_{\text{conf}} \cong H/a^2N$ is counterbalanced by an electrostatic force [6]. (The polyion is characterized by its total charge Q and its N monomer units with Kuhn length a . C_s is the ion concentration in solution, ℓ_B the Bjerrum length.) In a good solvent, a polymer is a Gaussian coil of thickness H and molecular area s .

In contrast to an isolated polyion, the planar grafted polyelectrolyte layer retains its counterions just as an infinitely charged plane [7]. The characteristic thickness of the counterion cloud Λ near the charged surface is given by $\Lambda \cong \ell_B^{-1}sa/Q$. When Λ is smaller than the brush thickness H , almost all counterions are localized inside the brush. Also, the screening length related to the counterion density in the brush, $r_D \cong (\ell_B Q/sH)^{-1/2}$, is smaller than its thickness H . Therefore, the decay of the counterion density from a mean value Q/sH inside the brush to zero occurs in a narrow region of thickness $r_D \ll H$ at the brush/solution interface, the corresponding amount of charge separated equals approximately Qr_D/H . The electrostatic force of this “capacitor” yields an electrostatic stretching force $f_{e1} \cong (Qr_D/H)^2/s \cong Q/H$. Equating electrostatic and conformational energy gives a large brush thickness $H \cong a(QN)^{1/2}$. The independence of H on the grafting density is a very unusual feature known only for the osmotically swollen polyion brush.

The salted brush occurs when the ion concentration C_s in solution approaches the one in the brush. Then, the “capacitor” thickness is given by $r_{Ds} = (\ell_B C_s)^{-1/2}$ with the amount of charge separated Qr_{Ds}/H , yielding an electrostatic force $f_{e1} \cong (Qr_{Ds}/H)^2/s \cong (Q/H)^2/sC_s$. Now, the equilibrium thickness shrinks $H \cong N(N/Q)^{-2/3}(sC_s)^{-1/3}$. To compare this prediction with the experiment, it is necessary to consider the finite volume of both the polymer and ions [8]. Therefore, the salt concentration C_s is to be replaced by the effective volume $v_{\text{eff}} = v + 1/(4\Phi_s Q^2/N^2)$ (with $v = 1/2$ as the excluded volume parameter of the polymer). Then, the predicted power law is $H \propto (sv_{\text{eff}})^{-1/3}$, with $\Phi_s = V_{\text{salt}}/V_{\text{monomer}}$, the volume fraction of the salt concentration as fitting parameter.

Materials and methods.—The block copolymer poly(ethyl ethylene)₁₁₄poly(styrene sulfonic acid)₈₃ (PEE₁₁₄-PSS₈₃) is chosen because bulk PEE is fluid at room temperature. The x-ray setup is home built [10,11] with a Cu anode ($\lambda = 1.54 \text{ \AA}$). In x-ray experiments, the

index of refraction n depends linearly on the electron density ρ and known constants (the Thomson radius r_0 , wavelength λ) $n = 1 - r_0\rho\lambda^2/2\pi$ and deviates only by $\approx 10^{-5}$ from 1. Therefore, approximations are possible, and the reflectivity can be seen as the Fresnel reflectivity R_F of an infinitely sharp interface modulated by interference effects from the thin surface layer [12].

$$\frac{R}{R_F} = \left| \frac{1}{\rho_{\text{sub}}} \int \rho'(z)e^{iQ_z z} dz \right|^2, \quad (1)$$

where ρ_{sub} is the electron density of the bulk phase, $\rho'(z)$ the gradient of the electron density along the surface normal, and Q_z the wave vector transfer normal to the surface. For clean water, $\rho_{\text{sub}} = 0.334 e^-/\text{\AA}^3$, it increases for concentrated ion solutions to $\rho_{\text{sub}} = 0.364 e^-/\text{\AA}^3$ (1M CsCl). The electron density profiles were calculated first by an indirect Fourier transform of Eq. (1) [13]. Yet to quantify molecular parameters, the exact matrix formalism is used. The monolayer is parameterized as consisting of different slabs (each with an electron density and a thickness, also a roughness parameter is necessary). The thus obtained electron density profiles coincide within error with the profiles obtained by indirect Fourier transform [10]. To eliminate correlated parameters, an interdependency analysis is performed [14]. The cation volume was extrapolated by comparing the respective volume increase of CsCl (NaCl, KCl), and HCl solutions.

Results.—To prepare a monolayer an appropriate amount of a $\text{CHCl}_3:\text{COOH}$ (3:1) solution with dissolved polymer (3 mg/ml) is spread on the water surface. After 10 minutes equilibration time isotherms are measured. The monolayer is stable, isotherms are reversible, if not indicated otherwise [cf. inset in Fig. 1(a)]. Always, a sudden break in the slope indicative of a phase transition is observed, whose position (π_c, A_c) depends on the subphase conditions [11]. Furthermore, at high ionic strength ($C_s > 0.1M$) a second phase transition appears (π_s) . Yet, in the intermediate range $\pi_c < \pi < \pi_s$ the isotherm indicates slow relaxation processes. To vary the molecular area s , x-ray experiments are taken along the isotherm.

The corresponding normalized x-ray reflectivity curves are structured and show some typical features: At low Q_z , a thick layer (the PSS block) causes interference, a narrow maximum followed by a shallow minimum is found. On monolayer compression, the contrast improves, the shallow minimum moves slightly to the left, indicating thickening. A thinner layer (the PEE block) causes the broad minimum at high Q_z , which shifts on compression.

The deduced electron density profiles are shown in Fig. 1(b). In the exact matrix formalism, four different slabs are necessary [11]: one for the PEE block, three for the PSS block. Just beneath the hydrophobic block always a thin layer ($\approx 12 \text{\AA}$) of high electron density is found (PSS1-slab). The long part of the polyelectrolyte brush is described by the PSS3 slab. PSS2 is numerically

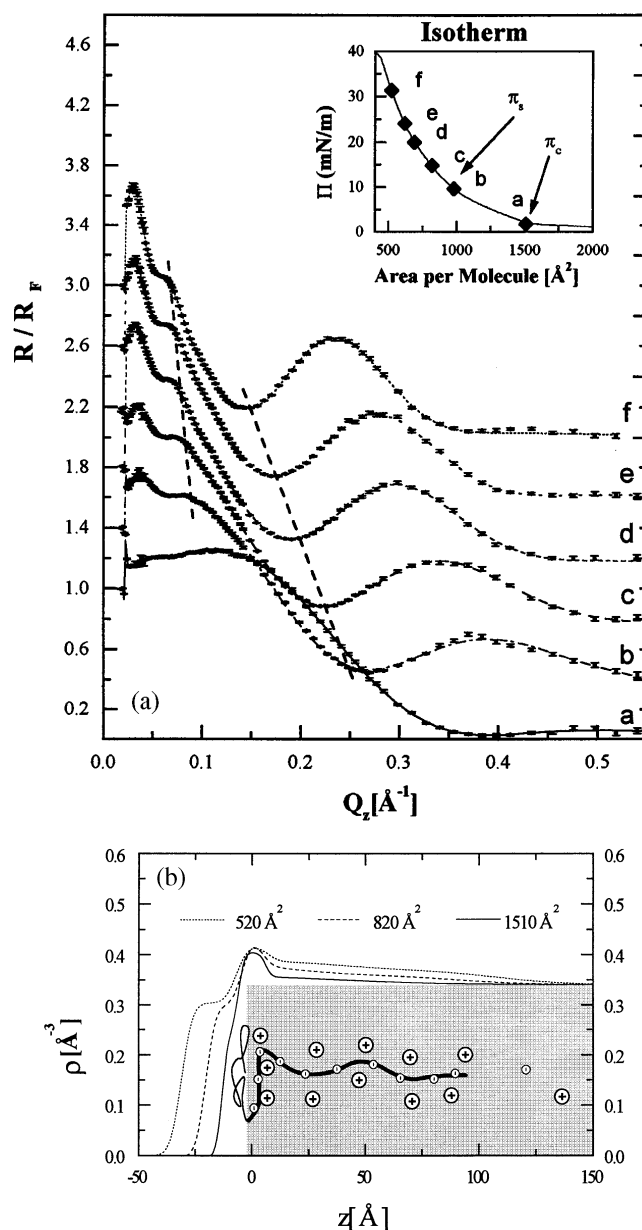


FIG. 1. (a) Normalized x-ray reflectivity measurements of the block copolymer $\text{PEE}_{114}\text{PSS}_{83}$ on a subphase containing 0.5 M KCl taken along the isotherm (shown in the inset) at different molecular areas labeled a–f. The full lines are simulated curves, from which the electron-density profile is deduced. For clarity, each reflectivity curve is displaced by 0.5. (b) The deduced electron density profiles for the molecular area indicated [curves a, c, and f from (a)]. The corresponding amphiphilic block copolymer is sketched to scale.

necessary to account for the slope change. Note, that the polyelectrolyte block is much longer, even though it exhibits the shorter contour length.

For all subphase conditions investigated, the hydrophobic block behaves as a nm-thick melt (cf. Fig. 2): its thickness d_{PEE} increases linearly with the grafting density. The slope is the one expected from the bulk

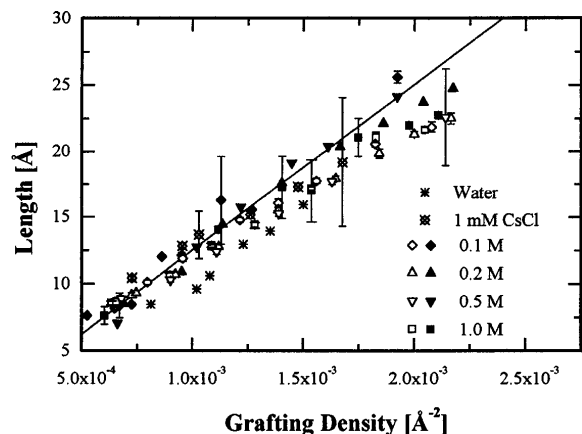


FIG. 2. Thickness of the hydrophobic PEE block as obtained from the electron-density profile for various subphase salt concentrations. The straight line is calculated under the assumption that the hydrophobic block exhibits the same mass density as the bulk phase.

density, which furthermore coincides with the measured electron density [15].

The polyion block shows more complex behavior. On clean water the brush length is constant [11] as expected for an osmotically swollen brush. Another predicted feature is stoichiometric counterion incorporation. Figure 3 shows normalized x-ray reflectivity curves of the monolayer at the same molecular area on diluted salt solutions. The contrast improves with $\text{Cs}^+ > \text{K}^+ > \text{Na}^+ > \text{H}^+$, i.e., with increasing electron density of the cation, while the position of the minima remains the same (constant thickness).

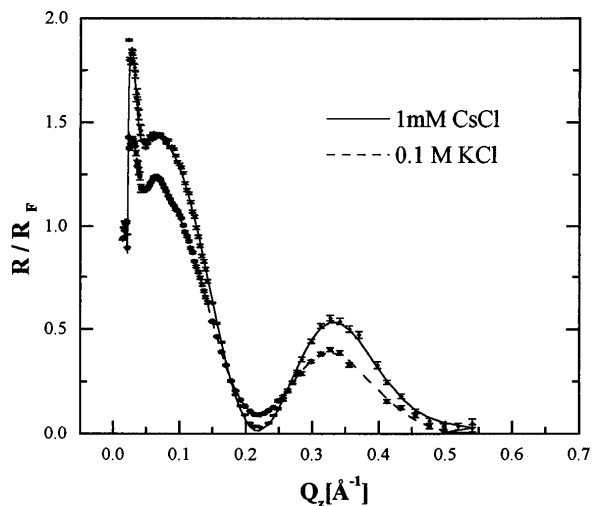


FIG. 3. Normalized x-ray reflectivity measurements of the block copolymer $\text{PEE}_{114}\text{PSS}_{83}$ at an area per molecule of 780 \AA^2 on 0.1 M KCl and 0.001 M CsCl. The increased contrast on CsCl solution indicates Cs^+ incorporation into the brush, whose thickness is the same. The full lines are simulated curves.

The model of stoichiometric ion incorporation is verified quantitatively by integrating along the brush: The brush volume, $V = s \int_{\text{brush}} dz$, and all the electrons in the brush, $N = s \int_{\text{brush}} \rho(z) dz$, are calculated. Since the monomer and counterion volume (electrons) are known, the excess volume (electrons) are attributed to water in the brush. Within 15%, the assumption of stoichiometric counterion incorporation appears to be valid. Depending on the grafting density, there are 40 to 65 water molecules per monomer in the brush. Yet in the PSS1-slab (the part of the PSS-chain which lays flat at the PEE/PSS interface) the polyelectrolyte is extremely concentrated ($6 \pm 1 \text{ H}_2\text{O}$ per monomer). Interestingly, in the case of the 0.001 M CsCl subphase (i.e., 1 CsCl for 55 000 water molecules), the Cs^+ concentration in the brush exceeds the one in solution by 3 orders of magnitude.

As expected, we find brush shrinking at high salt, for instance on a 0.5 M KCl subphase (cf. Fig. 1). To quantify this behavior, the thickness H as a function of the molecular area s is plotted for various salt concentrations [Fig. 4(a)]. As predicted for the salted brush phase, we find the power law with the exponent $1/3$ for salt concentrations exceeding 0.1 M and high grafting densities, independent of the kind of cation we use. Still, counterion incorporation is stoichiometric. Also, the theoretically predicted master curve is found, $H \propto (sv_{\text{eff}})^{-1/3}$, if we use $\Phi_s = V_{\text{salt}}/V_{\text{monomet}} = 1.5$ for both CaCl and KCl [cf. Fig. 4(b)], which is reasonable considering the experimental value of $\Phi_s = 0.25$.

At very high salt and low grafting density the polyelectrolyte brush appears to collapse with a much steeper power law than predicted. Indeed, the brush length is reduced by as much as a factor of 3. Yet, this collapse region is difficult to quantify, it corresponds in the isotherm to the intermediate compressed phase $\pi_c < \pi < \pi_s$, with its slow relaxation processes.

Discussion.—The transition from the osmotically swollen to the salted brush as indicated by shrinking, starts at $\approx 0.1 \text{ M}$ monovalent salt. Yet, the cation concentration in the brush is about 1 M . This suggests in the framework of the model outlined above, that about 10% of the counterions are freely mobile within the brush, the majority is bound to the polyelectrolyte, a number far exceeding Manning condensation [5]. This yields a Debye-screening length of $r_D \approx 10\text{--}15 \text{ \AA}$ which is indeed much smaller than H (120 \AA). Unexpected, and from the point of x-ray contrast fortunate, is the fact that the cations, especially the electron-rich Cs^+ , replace the protons in the polyelectrolyte brush, even though the counterion concentration may exceed the bulk concentration by more than 3 orders of magnitude. Additionally, we find a strong attraction between the hydrophobic grafting interface and the brush.

Conclusion.—The polyelectrolyte brush phases predicted theoretically, namely the osmotic brush phase and the salted brush phase are found experimentally for

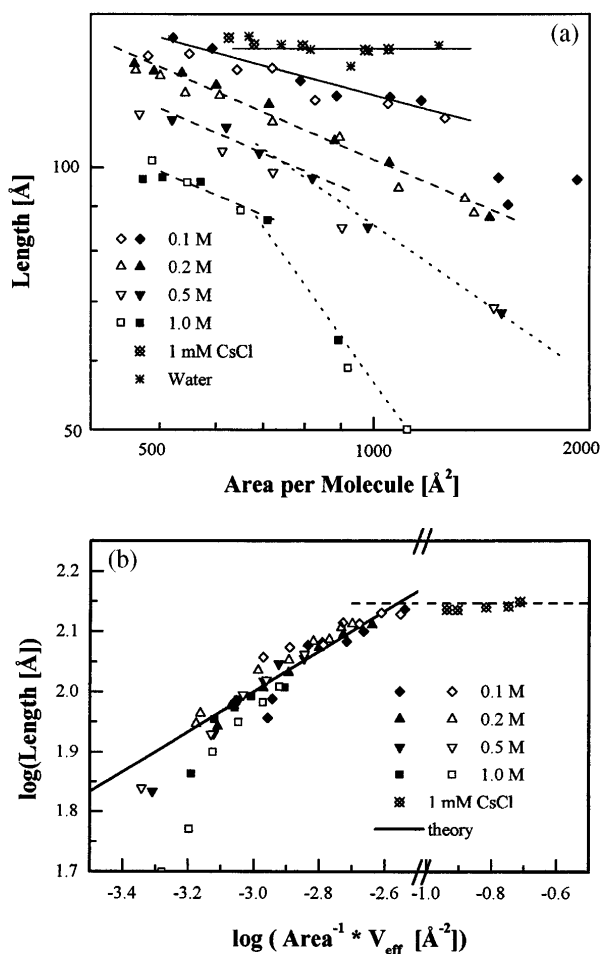


FIG. 4. (a) The thickness of the polyelectrolyte part of the monolayer ($H = d_{\text{PSS1}} + d_{\text{PSS2}} + d_{\text{PSS3}}$) as function of the area/molecule measured at the subphase conditions as indicated. Full symbols refer to KCl, open to CsCl. (b) The polyelectrolyte brush thickness as a function of the product of molecular area and an effective volume parameter, which is proportional to the salt concentration. The straight line is the theoretically expected power law for the salted brush, the dashed line indicates the constant thickness of the osmotically swollen brush.

medium length polymers. For both phases, the counterion incorporation is stoichiometric, a useful feature to optimize x-ray contrast. Finally, we have demonstrated that each block of an amphiphilic copolymer at the air/water interface behaves as predicted theoretically: either a liquid nm-thick melt or a polyelectrolyte brush.

C. A. H. enjoyed many discussions with Helmut M \ddot{o} hwald and Manfred Schmidt. Furthermore, we appreciate the financial support of the DFG (He 1616/7-1,2,3; F \ddot{o} 246/2-1,2).

*To whom correspondence should be addressed.

- [1] G. J. Fleer, M. A. Cohen-Stuart, J. M. H. M. Scheutjens, T. Cosgrove, and B. Vincent, *Polymers at Interfaces* (Chapman and Hall, London, 1993).
- [2] J. N. Israelachvili, *Intermolecular and Surface Forces* (Academic Press, London, 1991); F. Evans and H. Wennerstr \ddot{o} m, *The Colloidal Domain: Where Physics, Biology, and Technology Meet* (VCH, Weinheim, New York, 1994).
- [3] S. Alexander, *J. Phys. (Paris)* **38**, 983 (1997); P.-G. de Gennes, *Macromolecules* **13**, 1069 (1980).
- [4] S. T. Milner, *Science* **251**, 905 (1991).
- [5] S. F \ddot{o} rster and M. Schmidt, *Polyelectrolytes in Solution*, in *Physical Properties of Polymers* (Springer-Verlag, Berlin, 1995), pp. 51–133.
- [6] P. Pincus, *Macromolecules* **24**, 2912 (1991).
- [7] O. V. Borisov, E. B. Zhulina, and T. M. Birshtein, *Macromolecules* **27**, 4795 (1994); E. B. Zhulina, T. M. Birshtein, and O. V. Borisov, *Macromolecules* **28**, 1491 (1995).
- [8] R. Israels, F. A. M. Leermakers, G. J. Fleer, and E. B. Zhulina, *Macromolecules* **27**, 3249–3261 (1994).
- [9] Y. Mir, P. Auroy, and L. Auvray, *Phys. Rev. Lett.* **75**, 2863–2866 (1975); P. Guenoun, A. Schlachli, D. Sentenac, J. W. Mays, and J. J. Benattar, *Phys. Rev. Lett.* **74**, 3628–3631 (1995).
- [10] H. Baltes, M. Schwendler, C. A. Helm, and H. M \ddot{o} hwald, *J. Colloid Interface Sci.* **178**, 135–143 (1996); M. Ibn-Elhaj, H. Riegler, H. M \ddot{o} hwald, M. Schwendler, and C. A. Helm, *Phys. Rev. E* **56**, 1844–1852 (1997).
- [11] H. Ahrens, S. F \ddot{o} rster, and C. A. Helm, *Macromolecules* **30**, 8447–8452 (1997).
- [12] P. S. Pershan and J. Als-Nielsen, *Phys. Rev. Lett.* **52**, 759 (1984); J. Als-Nielsen, *Solid and Liquid Surfaces Studied by Synchrotron X-Ray Diffraction*, in *Structure and Dynamics of Surfaces*, edited by W. S. a. W. Blanckenhagen (Springer, New York, 1986).
- [13] J. S. Pederson and I. W. Hamley, *J. Appl. Cryst.* **27**, 36–49 (1994); J. S. Pederson, *J. Appl. Cryst.* **25**, 129–145 (1992).
- [14] A. Asmussen and H. Riegler, *J. Chem. Phys.* **104**, 8159–8164 (1996).
- [15] H. Baltes, M. Schwendler, C. A. Helm, R. Heger, and W. A. Goedel, *Macromolecules* **30**, 6633–6639 (1997).